



## MAIN TEXT ARTICLE

# The influence of left ventricular assist device inflow cannula position on thrombosis risk

Mojgan Ghodrati<sup>1,2</sup> | Alexander Maurer<sup>1,2</sup> | Thomas Schlöglhofer<sup>1,2,3</sup> |  
Thananya Khienwad<sup>1</sup> | Daniel Zimpfer<sup>3</sup> | Dietrich Beitzke<sup>4</sup> | Francesco Zonta<sup>5</sup> |  
Francesco Moscato<sup>1,2</sup> | Heinrich Schima<sup>1,2,3</sup> | Philipp Aigner<sup>1,2</sup>

<sup>1</sup>Center for Medical Physics and Biomedical Engineering, Medical University of Vienna, Vienna, Austria

<sup>2</sup>Ludwig Boltzmann Institute for Cardiovascular Research, Vienna, Austria

<sup>3</sup>Department for Cardiac Surgery, Medical University of Vienna, Vienna, Austria

<sup>4</sup>Department of Biomedical Imaging and Image Guided Therapy, Medical University of Vienna, Vienna, Austria

<sup>5</sup>Institute of Fluid Dynamics and Heat Transfer, Technical University of Vienna, Vienna, Austria

## Correspondence

Philipp Aigner, Center for Medical Physics and Biomedical Engineering, Medical University of Vienna, Währinger Gürtel 18, AKH-4L, A-1090 Vienna, Austria.  
Email: philipp.aigner@meduniwien.ac.at

## Funding information

Oesterreichische Nationalbank, Grant/Award Number: 17314; Österreichische Forschungsförderungsgesellschaft, Grant/Award Number: 858060 (M3dRES Additive Manufacturing for Medical)

## Abstract

The use of left ventricular assist devices (LVADs) as a treatment method for heart failure patients has been steadily increasing; however, pathological studies showed presence of thrombi around the HeartWare ventricular assist device inflow cannula (IC) in more than 95% of patients after device explantation. Flow fields around the IC might trigger thrombus formation and require further investigation. In this study flow dynamics parameters were evaluated for different patient geometries using computational fluid dynamics (CFD) simulations. Left ventricular (LV) models of two LVAD patients were obtained from CT scans. The LV volumes of Patient 1 (P1) and Patient 2 (P2) were 264 and 114 cm<sup>3</sup> with an IC angle of 20° and 9° from the mitral-IC tip axis at the coronal plane. The IC insertion site at the apex was central for P1, whereas it was lateral for P2. Transient CFD simulations were performed over 9 cardiac cycles. The wedge area was defined from the cannula tip to the wall of the LV apex. Mean velocity magnitude and blood stagnation region (volume with mean velocity <5 mm/s) as well as the wall shear stress (WSS) at the IC surface were calculated. Cardiac support resulted in a flow mainly crossing the ventricle from the mitral valve to the LVAD cannula for P2, while the main inflow jet deviated toward the septal wall in P1. Lower WSS at the IC surface and consequently larger stagnation volumes were observed for P2 (P1: 0.17, P2: 0.77 cm<sup>3</sup>). Flow fields around an LVAD cannula can be influenced by many parameters such as LV size, IC angle, and implantation site. Careful consideration of influencing parameters is essential to get reliable evaluations of the apical flow field and its connection to apical thrombus formation. Higher blood washout and lower stagnation were observed for a central implantation of the IC at the apex.

## KEYWORDS

apical washout, intraventricular flow pattern, left ventricle assist device, thrombosis risk

Presented in part at the 27th Congress of the International Society for Mechanical Circulatory Support, held October 21-23, 2019 in Bologna, Italy.

This is an open access article under the terms of the Creative Commons Attribution-NonCommercial-NoDerivs License, which permits use and distribution in any medium, provided the original work is properly cited, the use is non-commercial and no modifications or adaptations are made.

© 2020 The Authors. *Artificial Organs* published by International Center for Artificial Organ and Transplantation (ICAOT) and Wiley Periodicals LLC.

## 1 | INTRODUCTION

Mechanical circulatory support (MCS) therapy has progressively improved over the last decades and survival rates of patients with left ventricular assist devices have continuously increased.<sup>1</sup> Nevertheless, thrombogenicity of ventricular assist devices (VADs) remains a relevant problem and is closely linked to adverse events. Strokes, one of the most devastating complications,<sup>2,3</sup> are probably caused by thrombus depositions in the pump,<sup>4-6</sup> the inflow cannula<sup>7</sup> and outflow graft, and thrombi within the supported ventricle itself (Figure 1A).<sup>8-10</sup> The development of thrombosis and those depositions might be explained by the Virchow's triad of stasis, endothelial injury, and hypercoagulability.<sup>11</sup> Nonphysiological intraventricular flow patterns<sup>12,13</sup> in VAD patients create regions of stagnation at the site of the VAD.<sup>14,15</sup> Thrombus growth has been revealed on the outer surface of the HeartWare ventricular assist

device (HVAD) (Medtronic-HeartWare, Minneapolis, MN) inflow cannula (IC) in 33%-100% of cases<sup>16-18</sup> at the time of cardiac transplantation or autopsy. Multiple critical reasons for this are suspected, including patient factors (eg, intrinsic hypercoagulability, hypertension), management factors (eg, the anticoagulation regimen), the orientation of the IC to the mitral valve,<sup>19</sup> the size of the ventricle,<sup>20,21</sup> the insertion depth of the IC due to the left ventricle (LV) wall thicknesses,<sup>22,23</sup> the structure of outer surface of the cannula,<sup>7,24</sup> and positioning of the cannula.<sup>16,25-27</sup>

A potential additional cause for IC thrombus development might be a short distance between IC and ventricular septum. Based on photographs (Figure 1B) following cardiac transplantation or VAD explantation, a shorter distance to the septum showed a greater probability for an increase in thrombus formation or adhesion not only at this narrow distance, but also along the whole circumference.

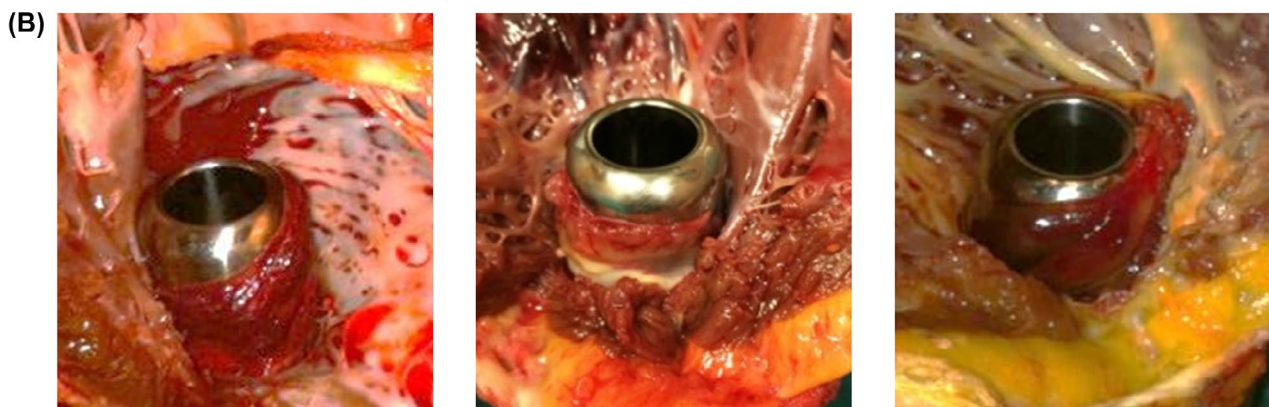
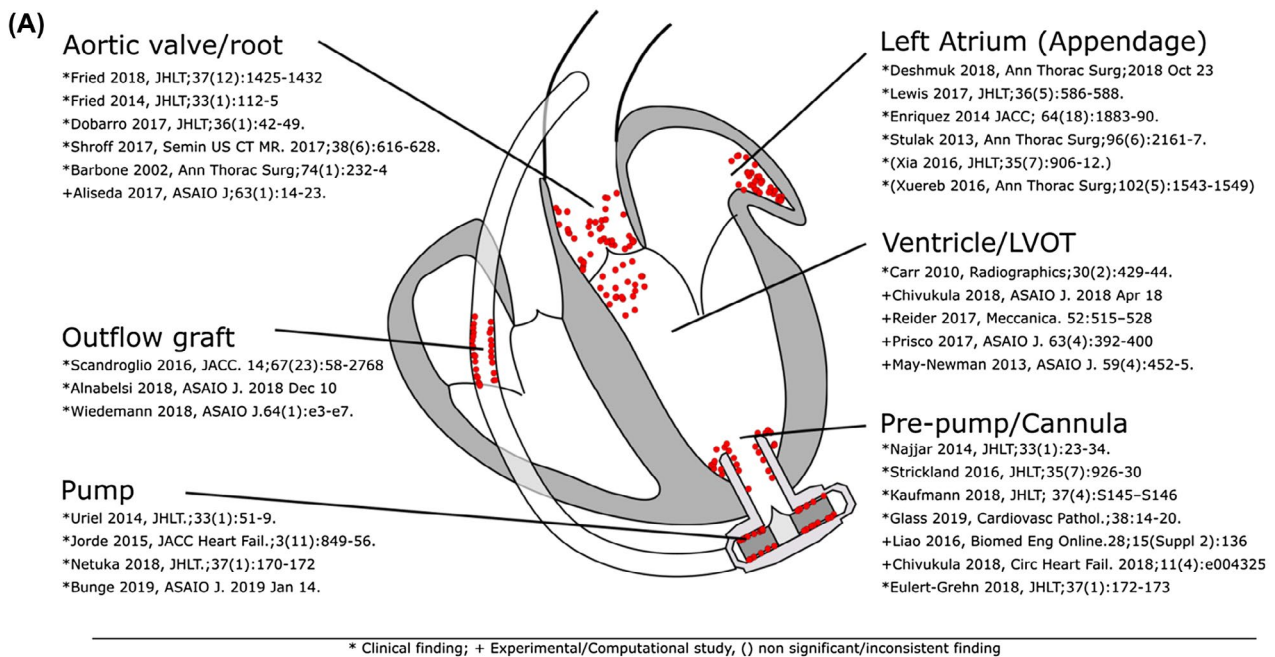


**FIGURE 1** A, The locations of the thrombus formation in the LVAD-assisted heart and B, thrombus growth around the LVAD IC at the time of cardiac transplant [Color figure can be viewed at [wileyonlinelibrary.com](http://wileyonlinelibrary.com)]



Therefore, this study aimed to investigate the apical flow field and consequently the risk of thrombosis for patient-specific geometries with different cannula position. To this end, we performed computational fluid dynamics (CFD) simulations based on individual CT scans for cannula positions placed at a significant distance to the ventricular walls in the apex and compared them to implants with closer proximity to the ventricular walls.

## 2 | PATIENTS AND METHODS

### 2.1 | Patient clinical background

Computed tomography (CT) scans of two representative destination therapy patients suffering from dilated cardiomyopathy were included in this study (clinical background and patient data shown in Table 1). Although the ventricular volumes were different at 116 and 264 cm<sup>3</sup>, these values were

within the clinically reported range.<sup>28</sup> Both patients were treated according to current guidelines suggesting mean arterial pressures (<90 mm Hg), target INR values (2.0-2.5), and antiplatelet therapy (>81 mg aspirin).<sup>7</sup>

### 2.2 | Patient models

Three-dimensional LV models were reconstructed from CT data using Mimics inPrint 2.0, Mimics Research 20.0 (Materialise, Leuven, Belgium). As a first step, the region of interest inside the LV was selected (Figure 2A,B first column), resulting in a rough mask of the LV chamber. This mask was modified and corrected with a final confirmation of the validity of the segmented geometry by a radiologist. Then a 3-dimensional STL file was created (Figure 2A,B second column) and exported to 3-matics Research 13.0 (Materialise) where filtering processes such as smoothing and spike removal were applied. Then, the HVAD IC was

**TABLE 1** Patient data for the two analyzed HVAD patients

Patient	Patient 1	Patient 2
Gender	Male	Male
Therapy type	Destination therapy	Destination therapy
Age (yrs)	75	76
Size (m)	1.74	1.74
Weight (kg)	99	91
BMI (kg/m <sup>2</sup> )	32.7	30.1
INTERMACS at implant	INTERMACS 4	INTERMACS 3
Ejection fraction before implant (%)	32	17
Concurrent procedures	No concurrent procedure, no prior cardiac surgery, minimal-invasive hemi-sternotomy, HLM	Tricuspid valve repair, no prior cardiac surgery, median sternotomy, HLM
POD of CT scan	20	1844
Referral for CT	Prospective before rehabilitation	Suction
Pump speed (rpm)	2600	2800
INR at CT scan	2.4	2.3
MAP (mm Hg)	84	84
Pump flow (L/min)	4.2	5.1
Pump power (W)	4.3	4.8
Pump flow amplitude (L/min)	5.0	4.0
Aspirin (mg)	100	200
LVV (end systolic, cm <sup>3</sup> )	264	114
LVESD (cm)	6.2	4.6
Hemocompatibility-related events during follow-up	None (up to POD 699)	Multiple gastrointestinal bleeding events (up to POD 2650)

positioned in the surgical configuration. Geometrical information such as the LV volume, distance of the IC surface to the lateral and septal wall, and the deviation of the IC with respect to MV–IC axis (axis connecting the center of the MV to the center of the IC) were calculated from the segmented LV (Figure 2C).

### 2.3 | Meshing

An unstructured tetrahedral mesh with an element size of 0.6 mm at the LV surface and 1.2 mm in the LV volume was created (ANSYS Meshing 19.1, Ansys Inc., Canonsburg, PA, USA), close to the IC and at the transition zone between the sintered and polished parts of the cannula—a high-resolution mesh with an element size of 0.3 and 0.05 mm, respectively, in order to provide detailed insight into fluid behavior at these regions. A mesh independence study was performed and results can be found in the Appendix.

### 2.4 | Solver setting

The blood was modeled as a non-Newtonian fluid with a density of  $1060 \text{ kg/m}^3$  and a dynamic viscosity of  $0.0035 \text{ Pa}\cdot\text{s}$ . The simulations were performed with the pulsatile flow at the mitral inflow with a total duration of 9 cardiac cycles ( $7.02 \text{ seconds}$ )<sup>29</sup> (see Figure 2D). The simulations were initialized by 5 seconds of simulation to allow for adequate flow development<sup>29</sup> and were computed with a temporal resolution of 0.001 seconds. The pump cannula outlet was set as an outflow boundary condition.

An unsteady incompressible finite-volume solver (Ansys Fluent 19.1, Ansys Inc.) was used to solve the mass and momentum conservation equations with the laminar method applying the no-slip boundary condition. A pressure-based solver with second-order upwind scheme spatial discretization was selected for the pressure, momentum, and continuity equations. Convergence was achieved in each time step when the residuals were below  $10^{-3}$  for continuity,  $x$ ,  $y$ , and  $z$  velocity.

### 2.5 | Flow parameter evaluation

The intraventricular flow field was visualized using the scalar mean velocity magnitude. The wedge area was defined from the tip of the cannula to the apex (Figure 2A,B), due to the importance of the apical flow fields.

Wall shear stress (WSS) at the cannula surface was categorized at three levels: low nonphysiological range ( $\text{WSS} < 0.3 \text{ Pa}$ ) which is related to thrombus formation,<sup>30</sup> physiological range ( $0.3 < \text{WSS} < 9 \text{ Pa}$ ), and high

nonphysiological range ( $\text{WSS} > 9 \text{ Pa}$ ) which leads to von Willebrand factor (VWF) elongation.<sup>31</sup>

A stagnation region (SR) was defined to highlight any regions where low time-averaged shear rates are observed, based on the assumption that any particles traveling at less than  $5 \text{ mm/s}$  through the wedge area could possibly lead to thrombus formation due to clotting mechanisms which are activated at such low shear rates.<sup>32</sup>

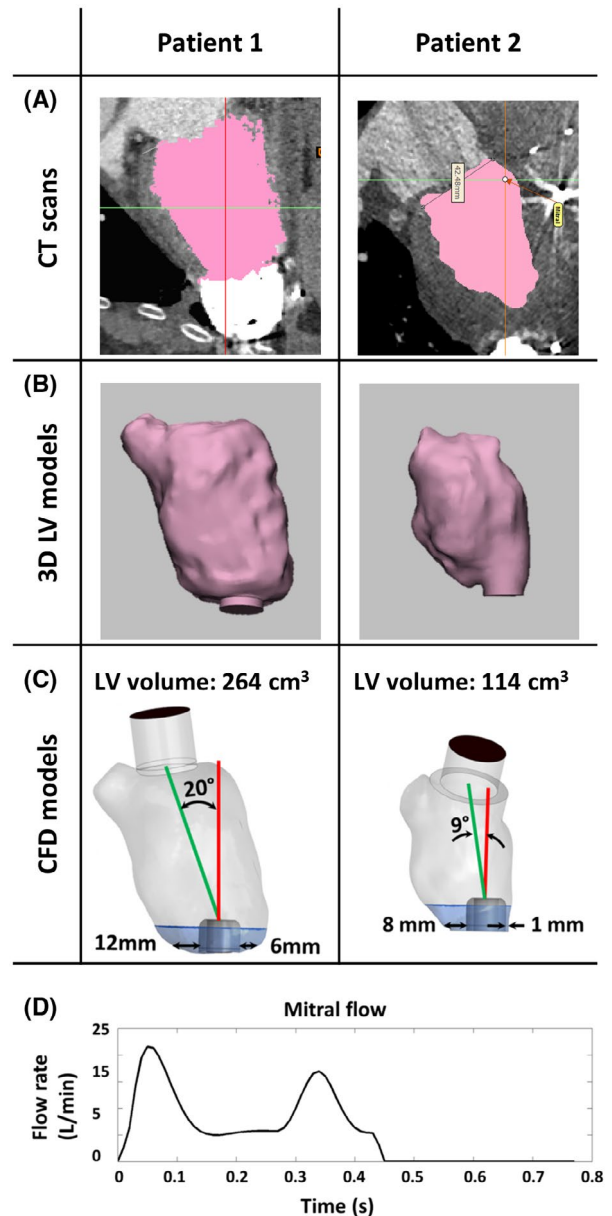


**FIGURE 2** A, CT scans and LV masks of both patients. B, 3D reconstructed LV models and C, final LV models with inserted IC. The cannula angle was determined through the deviation of the IC axis (red) from the MV–IC axis (green), along with the distance of the IC surface from the LV walls. D, The applied flow rate at the mitral valve [Color figure can be viewed at [wileyonlinelibrary.com](http://wileyonlinelibrary.com)]



### 3 | RESULTS

The ventricular flow field at the coronal plane showed different behavior for the patients: Velocity fields in the large ventricle showed a counter clockwise rotation, where the inflow jet was directed toward the septal side (Figure 3A; Patient 1), while for Patient 2 the main mitral inflow jet traveled straight toward the apex where the IC was implanted (Figure 3A; Patient 2).

In the larger LV, the main flow jet reached the apex of the LV at the septal side, where it travels around the IC and is then redirected upward along the ventricular wall on the lateral side of the IC (Figure 3B,C; Patient 1). This flow redirection leads to low nonphysiological shear stress distribution

at the backside of the IC surface (Figure 3B,C; Patient 1). However, this low WSS did not develop the large stagnation volume at the apical area (Figure 3D; Patient 1).

For the smaller LV and consequently shorter distance to the ventricular wall (Patient 2), part of the flow which is not transported directly through the IC reaches the septum wall and is redirected to the center of the LV without passing to the opposite side. Regarding WSS distribution, large areas with low nonphysiological WSS can be seen at the backside as well as the front side (Figure 3B,C; Patient 2), developing a large volume of stagnation at the apex of the LV (Figure 3D; Patient 2).

For both patients, high nonphysiological WSS was observed at the tip of the IC. Figure 4 shows the distribution of

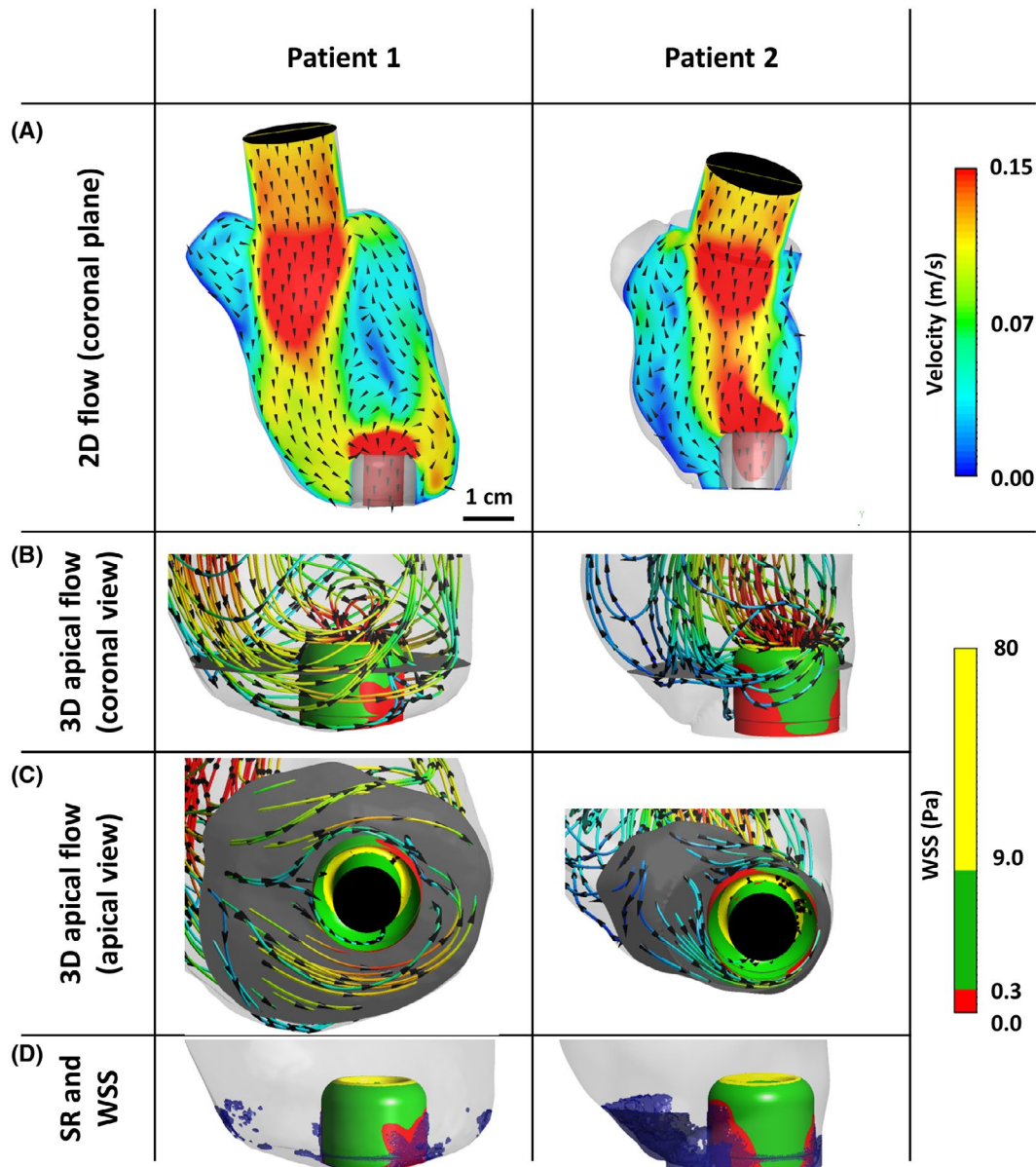


**FIGURE 3** A, 2D ventricular flow pattern visualized by mean velocity contour at coronal plane. 3D apical flow pattern visualized by velocity streamlines for B, coronal and C, apical view. D, WSS distribution at cannula surface and stagnation region [Color figure can be viewed at wiley onlinelibrary.com]

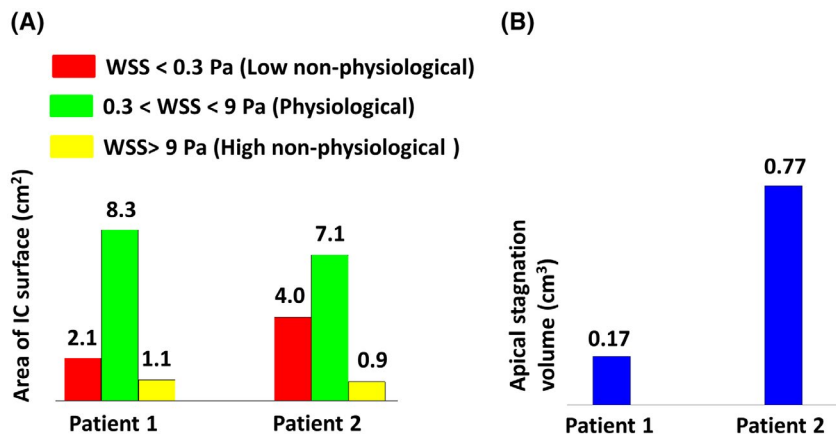


**FIGURE 4** A, The wall shear stress distribution at the cannula surface; B, the volume of stagnation at the apex [Color figure can be viewed at [wileyonlinelibrary.com](http://wileyonlinelibrary.com)]

the WSS at the IC surface in three categories as well as the volume of stagnation for both patients.

## 4 | DISCUSSION

The high reported prevalence of thrombi in the apical region of LVAD patients<sup>16-18</sup> highlights the necessity of a detailed evaluation of flow behavior in this region. Although several potential causes of thrombus growth during LVAD support have been reported,<sup>13,16-18,22,23,33</sup> this is the first study investigating the apical flow fields of LVAD patients to quantify the potential relationship of IC thrombus formation and IC to ventricular wall distance. The quantitative evaluation was based on the parameters which were already linked to thrombotic risk including SR and WSS.

The inflow jet was directed toward the septal wall for Patient 1 with the large LV. One possible reason for this behavior could be the large LV diameter and the angle of the MV–IC axis in the coronal plane. It can be seen in Figure 2A that the cannula deviated toward the lateral side by 20° from the MV–IC axis. Therefore the inflow jet has a curved shape directed toward the septum and reaches the apex of the LV at this side (apical separation point), where it traveled around the IC and was redirected to the center of the LV from the lateral wall (Figure 3). Although the cannula surface at the lateral side showed a low nonphysiological WSS distribution, the high apical washout with remarkable circular components prevents the development of stagnation region at these areas.

For Patient 2 (small distance between LV wall and IC), the angle of the IC with respect to the MV–IC axis was 9°, which enables the majority of the blood entering the LV through the MV to directly enter the cannula, with only a small part of the flow hitting the septal wall. The distance between the IC and lateral wall of the LV created a narrow gap because of the laterally displaced implantation of the cannula. Consequently blood flow around the cannula diminished and was instead

redirected to the center of the LV which highly reduced the washout around the cannula.

For both LV models, the transition zone of the sintered HVAD IC, which was already mentioned as the origin of thrombus formation,<sup>17</sup> was mainly within the low nonphysiological range and fully exposed to stagnating flow. High nonphysiological WSS already occurred at the cannula tip (Figure 3D), which can increase the risk of platelet activation when traveling through the pump cannula.

Thrombus formation and consequently thromboembolic adverse events are multifactorial phenomena,<sup>34</sup> including the type of LVAD,<sup>35-37</sup> blood stream infection,<sup>38</sup> anticoagulation therapy and blood pressure management,<sup>33,39,40</sup> the size of the LV,<sup>20,21,41</sup> and the inflow cannula insertion angle.<sup>14,19,42</sup> The results presented in this study emphasize that the implantation site of the inflow cannula also needs to be considered as a risk factor for thrombosis.

Stagnation at the apex was significantly increased with a cannula near the lateral wall compared to a central implantation of the cannula at the apex. Similar effects are expected for inflow cannulas close to other parts of the chamber wall, as the small distance blocks the blood circulation around the inflow cannula.

Further, in additional studies the effects of the MV–IC angle should be considered in more detail to be able to recommend optimal IC implantation.

## 5 | LIMITATION

Ventricular contraction is very limited in LVAD patients and therefore was not considered in this study but should be considered in future studies. However, ventricular contraction in VAD patients hardly happens at the apex, but mainly at the center of the ventricle.<sup>43</sup> Therefore only limited effects on apical flow are expected. The mitral valve leaflets were not included in the LV models, as its complex structure and interaction with cardiac contraction were not within the context of



this study and constitutes a separate field for further research. Finally, the number of two patients used in this study was very limited, yet the selected cases are good representatives of average patients and were carefully selected.

Among all the risk factors of ventricular thrombosis, this study addressed the implantation site of the inflow cannula and did not cover other contributing risk factors. Also due to the fact that both patients are still on LVAD support, the direct link of the found stagnation regions with the origin of the thrombus formation is missing. However, we consider this study a starting point for further investigations in this direction including MV–IC angle, mitral valve diameter, degree of support.

## 6 | CONCLUSION

The flow at the apex of the LVAD-supported ventricle and the thrombosis-related parameters are highly dependent on factors which change on a patient-to-patient basis. With the current data, circular blood washout and lower stagnation regions were observed for a cannula implantation at the apex with large parietal distances to the wall. Implantation of the IC close to the lateral/septal wall showed an increase in stagnation volume which is linked to an increase in thrombotic risk. This study shows that implantation and pump position can be an essential contributor to the adverse events profile of VAD pumps. However, considering the multifactorial nature of thromboembolic events, a further multiparameter analysis of the apical flow in a larger cohort could help to improve the understanding of the reasons for the high prevalence of thrombosis in this region.

## ACKNOWLEDGMENTS

This work was supported by the Vienna Scientific Cluster (VSC) Computer Network, the Project of the Jubiläumsfonds of the National Bank Austria Nr 17314 and the Austrian Research Promotion Agency (FFG): M3dRES Project Nr 858060.

## CONFLICT OF INTEREST

The authors declare that they have no conflicts of interest with the contents of this article.

## AUTHOR CONTRIBUTIONS

*Concept/design:* Ghodrati, Schima, Aigner

*Data analysis/interpretation:* Ghodrati, Aigner, Schima

*Drafting article:* Ghodrati, Aigner

*Critical revision of article:* Maurer, Schlöglhofer, Khienwad, Zimpfer, Beitzke, Zonta, Moscato, Schima, Aigner










*Approval of article:* Maurer, Schlöglhofer, Khienwad, Zimpfer, Beitzke, Zonta, Moscato, Schima, Aigner

*Statistics:* Ghodrati

*Funding:* Schima

*Data collection:* Ghodrati, Schlöglhofer, Aigner

## ORCID

Mojgan Ghodrati  <https://orcid.org/0000-0002-8475-3602>  
 Thomas Schlöglhofer  <https://orcid.org/0000-0003-4354-4860>  
 Thananya Khienwad  <https://orcid.org/0000-0002-4045-634X>  
 Daniel Zimpfer  <https://orcid.org/0000-0002-2185-4895>  
 Dietrich Beitzke  <https://orcid.org/0000-0003-3179-3827>  
 Francesco Zonta  <https://orcid.org/0000-0002-3849-315X>  
 Francesco Moscato  <https://orcid.org/0000-0003-0279-6615>  
 Heinrich Schima  <https://orcid.org/0000-0002-8003-7617>  
 Philipp Aigner  <https://orcid.org/0000-0002-3212-2112>

## REFERENCES

- Kirklin JK, Pagani FD, Kormos RL, Stevenson LW, Blume ED, Myers SL, et al. Eighth annual INTERMACS report: special focus on framing the impact of adverse events. *J Heart Lung Transplant.* 2017;36:1080–6.
- DeVore AD, Stewart GC. The risk of stroke on left ventricular assist device support. *JACC: Heart Failure.* 2017;5:712–4.
- Acharya D, Loyaga-Rendon R, Morgan CJ, Sands KA, Pamboukian SV, Rajapreyar I, et al. Analysis of stroke during support with continuous-flow left ventricular assist devices. *JACC: Heart Failure.* 2017;5:703–11.
- Uriel N, Han J, Morrison KA, Nahumi N, Yuzefpolskaya M, Garan AR, et al. Device thrombosis in HeartMate II continuous-flow left ventricular assist devices: a multifactorial phenomenon. *J Heart Lung Transplant.* 2014;33:51–9.
- Jorde UP, Aaronson KD, Najjar SS, Pagani FD, Hayward C, Zimpfer D, et al. Identification and management of pump thrombus in the HeartWare left ventricular assist device system. *JACC: Heart Failure.* 2015;3:849–56.
- Netuka I, Mehra MR. Ischemic stroke and subsequent thrombosis within a HeartMate 3 left ventricular assist system: a cautionary tale. *J Heart Lung Transplant.* 2018;37:170–2.
- Najjar SS, Slaughter MS, Pagani FD, Starling RC, McGee EC, Eckman P, et al. An analysis of pump thrombus events in patients in the HeartWare ADVANCE bridge to transplant and continued access protocol trial. *J Heart Lung Transplant.* 2014;33:23–34.
- Mehra MR, Stewart GC, Uber PA. The vexing problem of thrombosis in long-term mechanical circulatory support. *J Heart Lung Transplant.* 2014;33:1–11.
- Starling RC, Moazami N, Silvestry SC, Ewald G, Rogers JG, Milano CA, et al. Unexpected abrupt increase in left ventricular assist device thrombosis. *N Engl J Med.* 2014;370:33–40.
- Kirklin JK, Naftel DC, Kormos RL, Pagani FD, Myers SL, Stevenson LW, et al. Interagency Registry for Mechanically Assisted Circulatory Support (INTERMACS) analysis of pump thrombosis in the HeartMate II left ventricular assist device. *J Heart Lung Transplant.* 2014;33:12–22.
- Bagot CN, Arya R. Virchow and his triad: a question of attribution. *Br J Haematol.* 2008;143:180–90.
- Aigner P, Schweiger M, Fraser K, Choi Y, Lemme F, Cesarovic N, et al. Ventricular flow field visualization during mechanical circulatory support in the assisted isolated beating heart. *Ann Biomed Eng.* 2020;48:794–804.
- Reider C, Moon J, Ramesh V, Montes R, Campos J, Herold B, et al. Intraventricular thrombus formation in the LVAD-assisted heart studied in a mock circulatory loop. *Meccanica.* 2017;52:515–28.



14. May-Newman K, Marquez-Maya N, Montes R, Salim S. The effect of inflow cannula angle on the intraventricular flow field of the left ventricular assist device-assisted heart: an in vitro flow visualization study. *ASAIO J.* 2019;65:139–47.
15. Sonntag SJ, Lipinski E, Neidlin M, Hugenroth K, Benkowski R, Motomura T, et al. Virtual fitting and hemodynamic simulation of the EVAHEART 2 left ventricular assist device and double-cuff tipless inflow cannula. *ASAIO J.* 2019;65:698–706.
16. Strickland KC, Watkins JC, Couper GS, Givertz MM, Padera RF. Thrombus around the redesigned HeartWare HVAD inflow cannula: a pathologic case series. *J Heart Lung Transplant.* 2016;35:926–30.
17. Glass CH, Christakis A, Fishbein GA, Watkins JC, Strickland KC, Mitchell RN, et al. Thrombus on the inflow cannula of the HeartWare HVAD: an update. *Cardiovasc Pathol.* 2019;38:14–20.
18. Kaufmann F, Hörmandinger C, Potapov E, Krabatsch T, Falk V. HVAD thrombosis—searching for the Source. *J Heart Lung Transplant.* 2018;37:S145–6.
19. Chivukula VK, Beckman JA, Prisco AR, Dardas T, Lin S, Smith JW, et al. ventricular assist device inflow cannula angle and thrombosis risk. *Circ: Heart Failure.* 2018;11:e004325.
20. Chivukula VK, Beckman JA, Prisco AR, Lin S, Dardas TF, Cheng RK, et al. Small left ventricular size is an independent risk factor for ventricular assist device thrombosis. *ASAIO J.* 2019;65:152–9.
21. Pagani FD. Commentary: left ventricular size and left ventricular assist device support outcomes: bigger is better? *J Thorac Cardiovasc Surg.* 2019;157:2313–4.
22. Liao S, Neidlin M, Li Z, Simpson B, Gregory SD. Ventricular flow dynamics with varying LVAD inflow cannula lengths: in-silico evaluation in a multiscale model. *J Biomech.* 2018;72:106–15.
23. Schmid C, Jurmann M, Birnbaum D, Colombo T, Falk V, Feltrin G, et al. Influence of inflow cannula length in axial-flow pumps on neurologic adverse event rate: results from a multi-center analysis. *J Heart Lung Transplant.* 2008;27:253–60.
24. Soltani S, Kaufmann F, Vierecke J, Kretzschmar A, Hennig E, Stein J, et al. Design changes in continuous-flow left ventricular assist devices and life-threatening pump malfunctions. *Eur J Cardiothorac Surg.* 2015;47:984–9.
25. Aigner P, Schloeglhofer T, Plunger L, Beitzke D, Wielandner A, Schima H, et al. Relation between intraventricular HVAD position and pump thrombosis. *J Heart Lung Transplant.* 2018;37:S99–100.
26. Imamura T, Adatya S, Chung B, Nguyen A, Rodgers D, Sayer G, et al. Cannula and pump positions are associated with left ventricular unloading and clinical outcome in patients with HeartWare left ventricular assist device. *J Cardiac Fail.* 2018;24:159–66.
27. Bhama JK, Bansal A. Left ventricular assist device inflow cannula position may contribute to the development of HeartMate II left ventricular assist device pump thrombosis. *Ochsner J.* 2018;18:131–5.
28. Gupta S, Woldendorp K, Muthiah K, Robson D, Prichard R, Macdonald PS, et al. Normalisation of haemodynamics in patients with end-stage heart failure with continuous-flow left ventricular assist device therapy. *Heart Lung Circ.* 2014;23:963–9.
29. Ghodrati M, Khienwad T, Maurer A, Moscato F, Zonta F, Schima H, et al. Validation of numerically simulated ventricular flow patterns during left ventricular assist device support. *Int J Artif Organs.* 2020.
30. Rayz VL, Boussel L, Ge L, Leach JR, Martin AJ, Lawton MT, et al. Flow residence time and regions of intraluminal thrombus deposition in intracranial aneurysms. *Ann Biomed Eng.* 2010;38:3058–69.
31. Fraser KH, Zhang T, Taskin ME, Griffith BP, Wu ZJ. A quantitative comparison of mechanical blood damage parameters in rotary ventricular assist devices: shear stress, exposure time and hemolysis index. *J Biomech Eng.* 2012;134:081002.
32. Dintenfass L. Viscosity and clotting of blood in venous thrombosis and coronary occlusions. *Circ Res.* 1964;14:1–16.
33. Cho S-M, Hassett C, Rice CJ, Starling R, Katzan I, Uchino K. What causes LVAD-associated ischemic stroke? Surgery, pump thrombosis, antithrombotics, and infection. *ASAIO J.* 2019;65:775–80.
34. Li S, Beckman JA, Mahr C. Stroke in ventricular assist device patients: reducing complications and improving outcomes. *ASAIO J.* 2019;65:757–9.
35. Chiang YP, Cox D, Schroder JN, Daneshmand MA, Blue LJ, Patel CB, et al. Stroke risk following implantation of current generation centrifugal flow left ventricular assist devices. *J Card Surg.* 2020;35:383–9.
36. Goldstein DJ, Meyns B, Xie R, Cowger J, Pettit S, Nakatani T, et al. Third annual report from the ISHLT mechanically assisted circulatory support registry: a comparison of centrifugal and axial continuous-flow left ventricular assist devices. *J Heart Lung Transplant.* 2019;38:352–63.
37. Li S, Beckman JA, Cheng R, Ibeh C, Creutzfeldt CJ, Bjelkengren J, et al. Comparison of neurologic event rates among HeartMate II, HeartMate 3, and HVAD. *ASAIO J.* 2019.
38. Kanjanahattakij N, Horn B, Abdulhadi B, Wongjarupong N, Mezue K, Rattanawong P. Blood stream infection is associated with cerebrovascular accident in patients with left ventricular assist device: a systematic review and meta-analysis. *J Artif Organs.* 2018;21:271–7.
39. Cho S-M, Starling RC, Teuteberg J, Rogers J, Pagani F, Shah P, et al. Understanding risk factors and predictors for stroke subtypes in the ENDURANCE trials. *J Heart Lung Transplant.* 2020.
40. Tsiouris A, Heliopoulos I, Mikroulis D, Mitsias PD. Stroke after implantation of continuous flow left ventricular assist devices. *J Card Surg.* 2019;34:541–8.
41. Kawabori M, Kurihara C, Conyer R, Sugiura T, Critsinelis AC, Lee V-V, et al. A left ventricular end-diastolic dimension less than 6.0 cm is associated with mortality after implantation of an axial-flow pump. *J Thorac Cardiovasc Surg.* 2019;157:2302–10.
42. Sorensen EN, Kon ZN, Feller ED, Pham SM, Griffith BP. Quantitative assessment of inflow malposition in two continuous-flow left ventricular assist devices. *Ann Thorac Surg.* 2018;105:1377–83.
43. Addetia K, Uriel N, Maffessanti F, Sayer G, Adatya S, Kim GH, et al. 3D morphological changes in LV and RV during LVAD ramp studies. *JACC: Cardiovasc Imaging.* 2018;11:159–69.

## SUPPORTING INFORMATION

Additional Supporting Information may be found online in the Supporting Information section.

**How to cite this article:** Ghodrati M, Maurer A, Schloeglhofer T, et al. The influence of left ventricular assist device inflow cannula position on thrombosis risk. *Artif Organs.* 2020;44:939–946.  
<https://doi.org/10.1111/aor.13705>